

Zero-difference ambiguity blocking

Properties of satellite/receiver widelane biases

F. Mercier, *CNES*
D. Laurichesse, *CNES*

BIOGRAPHY

Flavien Mercier is a member of the precise orbit determination team at CNES, which produces the precise orbits for JASON and ENVISAT. He is a senior engineer in GPS processing for precise applications.

Denis Laurichesse is a member of the orbit determination service at CNES. He has been in charge of the Diogène GPS orbital navigation filter, and is now currently involved in navigation algorithms for GNSS systems.

1. INTRODUCTION

Precise GNSS applications (positioning, orbit determination, time transfer) use the phase measurements with integer ambiguity processing in order to reach the maximum accuracy. This is currently performed in geodetic precise applications using double difference processing. The double difference methods eliminate completely the clock information from the solutions. This is an advantage for global geodetic solutions, because it minimises drastically the size of the parameterisation and leads to an efficient ambiguity fixing process. However, other applications cannot benefit directly of integer ambiguity fixing due to this elimination: for example Precise Point Positioning or time transfer.

Thus it is very interesting to study the integer ambiguity properties at zero difference level. A first step was achieved on single difference measurements [1,2,3]. The complete ambiguity fixing has been performed on intermediate length baselines (a few hundred of kilometres). Then a complete formulation for zero difference modelling of GPS dual frequency measurements has been developed [4]. This formulation takes the phase measurements as the reference for the clocks offsets construction. These clocks offsets have interesting properties closely related to the ambiguity fixing properties.

The overall process depends on some system biases related to the widelane ambiguity [4,5]. An important result is the characterisation of these system biases. The objective in [5] was to characterise precisely all system biases related to zero-difference measurements. The integer ambiguities are a by-product in this case. The main result of these studies is that the system relative biases between pseudo-range and phase measurements

may have important variations. This characteristic was also observed for example between ionosphere-free combinations of pseudo-range and phase, even with floating ambiguities solutions [6].

In the present paper, the latest results obtained for the characterisation of the widelane satellite fractional delays are presented. These delays have been estimated for year 2007 on a daily basis. They allow a very efficient zero difference widelane blocking for any ground station (here only the Ashtech receiver were processed, the generalisation to other receiver technologies has been shown in [4]).

The application of these delays for the computation of integer phase clocks on a global network of 54 stations is also detailed.

2. GENERAL OVERVIEW OF THE FORMULATION

The complete solution of ambiguities at zero-difference level involves two steps [4]:

- the first step uses the four GPS elementary measurements (pseudo-range and phase on the two frequencies) to observe directly the difference between the two elementary ambiguities (widelane combination). Some system biases are necessary to define and identify (widelane fractional biases, which can also be seen as widelane clocks). The observation of the long term evolution of these biases is the first objective of the present study, together with the performance of the related widelane ambiguity blocking.

- when the difference between the two elementary ambiguities is known, it is possible to solve for the remaining ambiguity using only the model and the ionosphere-free phase combination. The equation set corresponds now to a single frequency system, without ionosphere propagation effects, and an equivalent wavelength of 10.7 cm. This allows a direct observation of the zero-difference ambiguities in the residuals when the models are accurate (typically 1-2 centimetres, which is possible in current positioning problem like ground station positioning). This was used to construct 'integer phase clocks' for time transfer [7] and for integer PPP [8,9].

2.1 FOUR OBSERVABLES EQUATION

In order to observe the zero-difference phase ambiguities, it is necessary to explicitly express all the system biases which are eliminated in the classic double-difference process. The equations for the four measurements of a geodetic receiver are (for example, case of an Ashtech receiver), for one receiver and one satellite :

$$\begin{aligned} P_1 &= D_1 + e + \Delta h_p + \Delta \tau_p \\ P_2 &= D_2 + \gamma e + \Delta h_p + \gamma \Delta \tau_p \\ \lambda_1 L_1 &= D_1 + \lambda_1 W - e + \Delta h + \Delta \tau - \lambda_1 N_1 \\ \lambda_2 L_2 &= D_2 + \lambda_2 W - \gamma e + \Delta h + \gamma \Delta \tau - \lambda_2 N_2 \end{aligned} \quad (1)$$

The left hand side corresponds to the pseudo-range and phase measurements on the two frequencies (rinex notations and units: P_1, P_2 pseudo-ranges on the two frequencies in meters, L_1, L_2 phase measurements in cycles). The right hand side corresponds to the model:

- λ_1, λ_2 : wavelength for the two frequency bands, $\gamma = \lambda_2^2 / \lambda_1^2$.
- D_1, D_2 : geometrical propagation distance between the respective phase centres including troposphere delay, relativistic effects, etc. W is the contribution of the wind-up effect (in cycles).
- e is the ionosphere delay on frequency 1 in meters.
- N_1, N_2 are the two carriers phase integer ambiguities in cycles.

The Δ operator represents the difference between the receiver value and the emitter value. For example, for the clock contribution for receiver i and satellite j , we have $\Delta h = h_i - h^j$ with h_i the receiver clock and h^j the emitter clock. In these equations, all system biases, including the clocks, are expressed in meters.

The system biases (receiver or emitter) are defined relative to the ionosphere free phase clock h for the phase, and relative to the ionosphere free pseudo-range clock h_p for pseudo-range equations. τ represents the bias between the two phase measurements in a similar way as the Time Group Delay τ_p which is defined on the pseudo-range measurements.

The biases $h - h_p, \tau, \tau_p$ are assumed to have slow and limited variations with time. This is a reasonable hypothesis, because various observed combinations of these biases have these characteristics, for example:

- mean TGD is very stable over long durations (see IGS values),
- ionosphere-free code and phase biases may have important variations (one meter), but on rather long durations (one day) [5,6],
- differences of τ for two receivers were observed on short baselines.

Figure 1 shows comparisons of the L_1 and L_2 residuals obtained on a very short baseline [3] (the two receivers i_0, i_1 use the same frequency reference). The hardware biases were not calibrated, so the global biases in these residuals are arbitrary. L1 residuals correspond to $(h_{i1} + \tau_{i1}) - (h_{i0} + \tau_{i0})$ and L2 residuals to $(h_{i1} + \gamma \tau_{i1}) - (h_{i0} + \gamma \tau_{i0})$. We see on this example that with the above definitions, the value $(\gamma - 1)(\tau_{i1} - \tau_{i0})$ may have variations up to 0.5 cycles in a few hours. This is due to the difference in the phase clocks observed on the two frequencies.

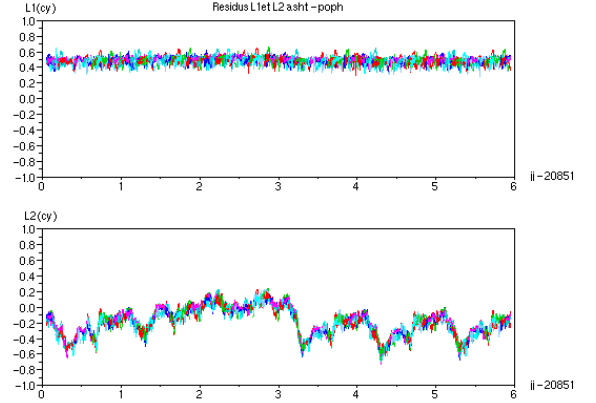


Figure 1: phase residuals on a very short baseline, common clock.

3. ZERO DIFFERENCE INTEGER WIDELANE AMBIGUITY SOLUTION

3.1 FORMULATION

The pseudo-range and phase widelane (also called Melbourne-Wübbena) combination $f(L_2 - L_1, P_1, P_2)$ is now constructed for each pass. This is the ionosphere and geometry free linear combination between the pseudo-range P_1 and P_2 and the difference of the phases L_1 and L_2 expressed in cycles (the subscripts correspond to the two frequencies). For each measurement of one pass between receiver i and satellite j this combination can be expressed as (neglecting the contribution of the difference $D_2 - D_1$ which is well below 0.1 cy for current antennas):

$$\begin{aligned} f(L_2 - L_1, P_1, P_2) &= -N_w + \mu_i - \mu^j \\ N_w &= N_2 - N_1 \end{aligned} \quad (2)$$

for all measurements of a pass between receiver i and emitter j

In these equations N_1, N_2, N_w are constant integer over the pass, and μ_i, μ^j are respectively the receiver i and satellite j widelane biases. μ_i and μ^j depend only on time. For the emitters, these values vary slowly with time, the variations are typically well below one cycle during one day. For the receivers, they are generally stable in good environmental conditions. In some cases,

variations up to a few cycles per hour have been observed for an outdoor test receiver [8].

Equations (2) can be solved on a global network at each epoch to obtain the rapid time variations of μ_i, μ^j [5]. The drawback of this approach is that an important network of stations is needed, because common views are necessary to observe all coefficients at each epoch (like in a standard network clock solution).

Here we only search a sufficiently accurate approximation of μ_i, μ^j in order to fix the values of N_w . Over a limited period and with good stations (a few days), the values of μ_i, μ^j are stable enough to replace equations (2) by averages over each pass and use constant or slowly varying values μ_i, μ^j .

$$\langle f(L_2 - L_1, P_1, P_2) \rangle_{pass} = -N_w + \mu_i - \mu^j \quad (3)$$

An iterative algorithm has been developed [9] to find one of the possible solutions for the μ_i, μ^j coefficients in the set of equations (3) and the corresponding N_w values.

All other possible solutions can then be expressed by $\mu_i + b + k_i, \mu^j + b + k^j$ with one integer k_i, k^j for each emitter or receiver, and one floating value b common to all (we can remark that this property is also valid for equation (2), but with a time varying b). When a solution μ_i, μ^j is chosen, all widelane ambiguities are defined for any receiver. These coefficients can be applied for any receiver of the same technology (for different technologies, further calibrations are needed due to different pseudo-range observables biases, for example between Ashtech and Trimble receivers [4]).

All these processing can be performed using only the receiver measurements files: no external model is necessary (broadcast orbits, station coordinates...).

3.2 RESULTS ON A GLOBAL NETWORK

Now a set of consistent N_w is constructed on a worldwide network of 54 stations over three days.

First, a set of constant μ^j is identified using only four stations (here the IGS stations, Ashtech receivers : usn3, brus, tidb, mcm4).

Second, these emitter values are applied in equation (2), to compute for each receiver a time varying $\mu_i(t)$ and one widelane ambiguity per pass.

Figure 2 shows the values of $f(L_2 - L_1, P_1, P_2) + \mu^j$ for receiver mets, for all measurements in a limited period of day 182 year 2007. These values correspond to $\mu_i(t)$

modulo 1 cycle, an integer value has been added on each pass in order to clarify the drawing.

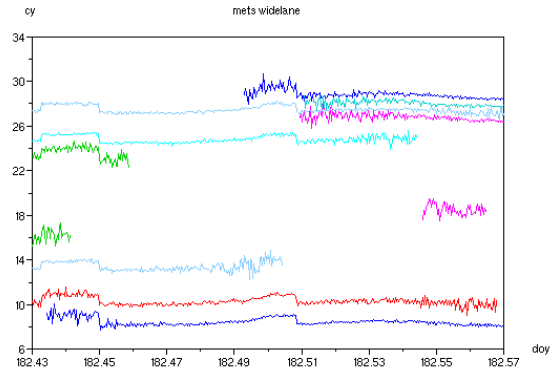


Figure 2: mets receiver widelane combination results, satellite widelane biases corrected

We see here that $\mu_i(t)$ may have rapid variations up to 1 cycle in a few minutes (data sampling is 30 s). This means that for such a receiver, it is necessary to take into account a non constant value of $\mu_i(t)$ to identify correctly the integer ambiguities N_w .

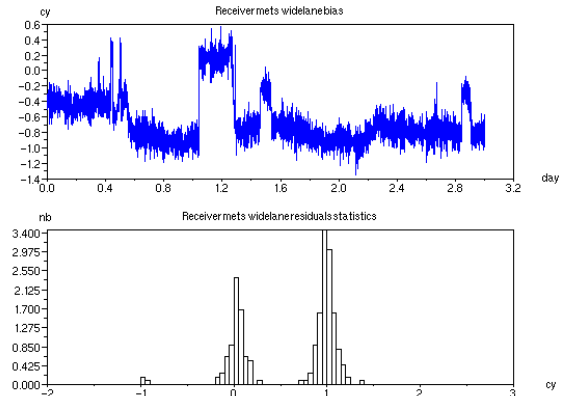


Figure 3: mets receiver, widelane fractional bias passes residuals statistic

Figure 3 shows the identified value of $\mu_i(t)$ and the statistics of $\langle f(L_2 - L_1, P_1, P_2) + \mu^j - \mu_i(t) \rangle_{pass}$ for station mets (only passes with more than 10 minutes length were used). The values stay close to 0, because for each pass the phase measurements were roughly aligned on the pseudo-range measurements with a constant integer correction for each pass. We see that almost all passes the ambiguities can be reliably fixed. Typically a threshold of 0.25 cycle is used in the current processing.

For almost all receivers there are no such jumps in $\mu_i(t)$. More frequently there are some fluctuations with 24 hours period, and amplitudes well below one cycle.

Figure 4 shows the statistics of $\langle f(L_2 - L_1, P_1, P_2) + \mu^j - \mu_i(t) \rangle_{pass}$ for the complete network for three days (days 182 to 184, 2007). The

chosen threshold value for blocking is ± 0.25 cycles. 99.4 % of the initial measurements are in a pass with a blocked widelane ambiguity.

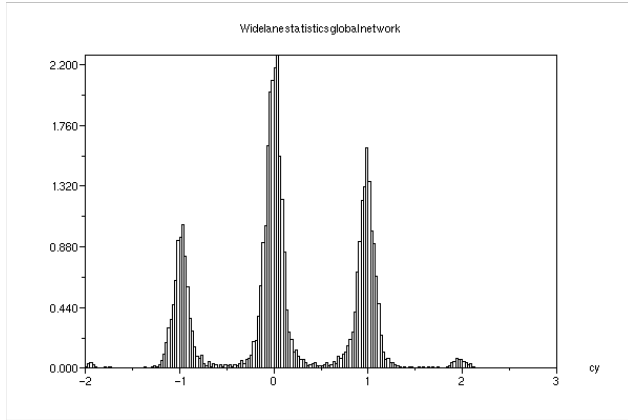


Figure 4: statistics of widelane ambiguities for the global network

3.3 SATELLITE WIDELANE FRACTIONAL BIASES

In the preceding paragraph, it was shown that the observed satellite fractional biases were sufficiently stable during three days to use a constant value. However, the change of these values must be analyzed for longer durations. Here, the fractional widelane biases are estimated for four reference receivers (*usn3*, *brus*, *mali*, *glps*) for year 2007. Receivers with stable μ_i are chosen in order to construct efficiently the daily solutions without solving for the receiver widelane bias at each epoch. The fractional biases are computed with the same process as above (equation (3)), with a three days sliding window. No constraint is applied between successive elementary solutions (only an integer correction is applied on two successive solutions to achieve a continuous behavior). The final μ^j value is assigned to the central day.

Figure 5 shows some satellite widelane fractional biases relative to the *usn3* receiver for year 2007. The results are shown for some block IIR satellites (numbers 11 to 16) and some block IIA satellites (numbers 3 to 8).

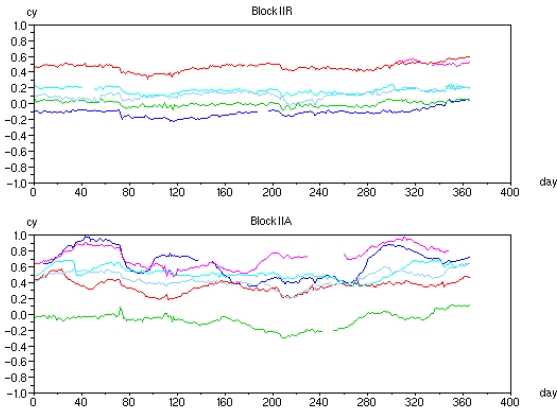


Figure 5: GPS satellite widelane fractional biases for year 2007

The biases for the block IIR satellites are very stable. We observe correlated variations between the different satellite biases which are probably due to *usn3* reference. For the block IIA satellites, the stability is not as good as for IIR satellites.

Figure 6 shows the results of the application of these satellite widelane fractional biases on the *brus* receiver measurements, for year 2007, for all passes longer than 2 hours (values of $\langle f(L_2 - L_1, P_1, P_2) \rangle_{pass} + \mu^j$, modulo 1).

The *brus* receiver widelane fractional bias evolution relatively to the chosen reference *usn3* is clearly visible. For a given day, the results are generally within an interval of ± 0.1 cycle. This shows that the precision of the mean satellite biases μ^j is better than 0.1 cycle. This means also that the widelane integer ambiguities can be identified for almost all passes using these daily μ^j values.

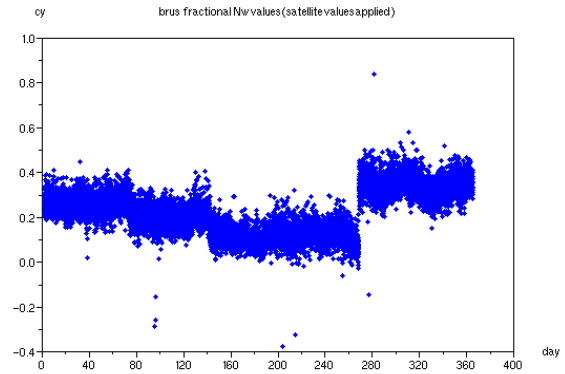


Figure 6: *brus* widelane fractional values corrected with μ^j

4. N1 ZERO DIFFERENCE AMBIGUITY RESOLUTION

4.1 REFERENCE EQUATIONS

Using equations (1), it is now possible to construct the ionosphere free code and phase observables, with the integer widelane corrections found above applied:

$$\begin{aligned} P_c &= D_c + \Delta h_p \\ Q_c &= D_c + \lambda_c W + \Delta h - \lambda_c N_1 \end{aligned} \quad (4)$$

$Q_c = \frac{\gamma \lambda_1 L_1 - \lambda_2 (L_2 + N_w)}{\gamma - 1}$ is the ionosphere free phase observable

$P_c = \frac{\gamma P_1 - P_2}{\gamma - 1}$ is the ionosphere free code observable

$D_c = \frac{\gamma D_1 - D_2}{\gamma - 1}$ is the ionosphere free geometric propagation (including troposphere effects)

N_1 is the remaining ambiguity to find, associated to the wavelength $\lambda_c = \frac{\gamma\lambda_1 - \lambda_2}{\gamma - 1}$.

Without restricting the generality of the equation, we can suppose that N_1 is small (for example by correcting Q_c with an integer number of λ_c in such a way that it is close to P_c).

We assume that the ephemeris and stations coordinates are precise enough to have an error below 1 centimeter for the geometric modeling (use of IGS solutions [10]). The remaining model parameter which has to be adjusted is the zenith troposphere delay. For each station, this delay is obtained by a standard PPP procedure with floating ambiguities.

The phase equation in (4) can now be rewritten as:

$$R_c = \Delta h - \lambda_c N_1 \quad (5)$$

This equation has to be solved for h_i (receiver) and h^j (emitter) at each epoch, and an integer value N_1 for each pass.

4.2 CLOCK AND AMBIGUITY SOLUTION

Equation (5) has a similar structure as (3). The solution is undetermined in two distinct ways:

- a reference clock must be constrained, because all equations involve differences between two clocks.
- each clock value can be changed with an integer number k of λ_c by correcting the corresponding ambiguities (passes with the corresponding receiver or emitter) with k . More generally, this property holds for all sets of clock values which cannot be connected with overlapping passes.

We can also remark that when the clocks values are defined, it is possible to check against the integer ambiguity value by computing $\frac{R_c - \Delta h}{\lambda_c}$ on each pass, with the available clock values.

The algorithm to find the ambiguity solution uses this property. Schematically, the current iteration is:

- initial integer clock solution (h_i, h^j)
- application on all passes by estimating $N_1 = - \left\langle \frac{R_c - (\Delta h)_n}{\lambda_c} \right\rangle_{pass}$, and construction of a set of integer ambiguity passes corresponding to $(N_1)_n$. In

order to have an efficient procedure, only the passes corresponding to a given set of epochs are processed, then the epochs are shifted and the process is repeated. This maintains the synchronization between the processed passes.

- estimation of a new clock solution $(h_i, h^j)_{n+1}$ by solving $\Delta h = R_c + \lambda_c (N_1)_n$ with the current set of blocked passes

The convergence is checked using the success rate of the blocking step. Typically, on the global network of 54 stations, the number of blocked passes is around 99 % (minimum elevation 10 degrees, minimum duration 1 hour, tolerance 0.25 cycles).

However, this process stops if there is a completely undefined clock (emitter or receiver) at the current step: in this case it is necessary to construct the initial current clock estimate using a reference pass. For example, for an undefined emitter clock h^j , the first estimation is given by using equation (5) with an arbitrary value for N_1 : $h^j = h_i - R_c$.

Also, the initialization phase of the process follows this procedure by using all the passes on a reference station at the initial epoch.

4.3 RESULTS

Table 1 summarises the results obtained for the global network (residuals rms, initial number of measurements with blocked widelane, ratio of N_1 blocking).

We remark on this table that GPS29 has significantly less blocked measurements than the other satellites. By checking the residuals, it appears that this is due to an anomaly at the beginning of day 184. This is confirmed by the flags of the IGS sp3 file, which drops to 5 for GPS 29 this day.

The eclipsing GPS IIA have also important rms values in the residuals. By checking the time histories, it appears that around the eclipses, there are important errors in the phase residuals which may reach ~7 centimetres. This means that the true centre of phase trajectory is not consistent with the theoretical one, and the order of magnitude is compliant with the current definitions of the x offsets for block IIA (27.9 cm). Figure 7 shows a zoom on the residuals of GPS10 around one eclipse period. We clearly see the beginning and the end of the yaw error of the model. We see also that the satellite makes more than a complete rotation, because the residuals reach 0 before the end of the eclipse and grow again until the end of the eclipse.

	rms (mm)	nb meas.	nb. bloc.
GPS01	7.7	9227	99.79 %
GPS02	9.1	8620	99.41 %
GPS03	8.8	8999	99.16 %
GPS04	9.1	9074	99.70 %
GPS05	7.8	8934	100.00 %
GPS06	8.1	8794	99.19 %
GPS07	8.5	9294	99.88 %
GPS08	10.5	8278	99.24 %
GPS09	9.7	8777	99.82 %
GPS10	12.3	8961	99.65 %
GPS11	9.2	9657	99.76 %
GPS12	9.6	9406	99.30 %
GPS13	8.5	8920	99.61 %
GPS14	8.4	8708	100.00 %
GPS15	-	-	-
GPS16	9.3	8663	99.97 %
GPS17	10.3	9255	99.64 %
GPS18	8.5	9192	99.40 %
GPS19	10.8	8836	99.73 %
GPS20	8.6	9529	99.79 %
GPS21	8.7	8601	100.00 %
GPS22	9.6	9298	99.76 %
GPS23	9.6	9130	99.26 %
GPS24	8.1	8836	99.89 %
GPS25	8.4	8540	100.00 %
GPS26	8.4	8484	99.60 %
GPS27	10.2	9076	99.74 %
GPS28	9.6	9390	99.52 %
GPS29	9.4	8149	96.71 %
GPS30	7.8	9038	99.81 %
GPS31	10.5	9358	99.85 %

Table 1 : statistics of the results
* : GPS IIA with eclipses

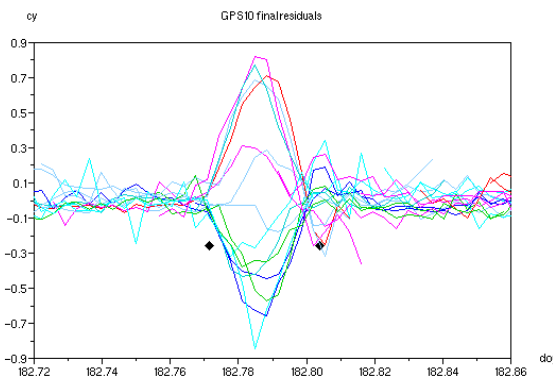


Figure 7: behavior of GPS10 during an eclipse
symbols are at beginning and end of eclipse

Figure 8 shows the results for station *alrt*: final residuals, initial residuals (obtained by computing $\frac{R_c - \Delta h}{\lambda_c}$ for each measurement, one arbitrary remaining ambiguity per pass), and the continuity of the passes (number of passes which extend between two successive epochs, blue curve is for the widelane, green is for N_1). Each colour corresponds to one GPS satellite. Figure 9 shows the corresponding data for GPS01. Each colour corresponds to one station.

This shows that the widelane zero-difference ambiguities are correct (incorrect blocking leads to one cycle error in the widelane which produces half cycles in

the final N_1 blocking). Thanks to the precision of the inputs (igs ephemeris, PPP solutions for troposphere, estimation of the widelane ambiguity), almost all integer N_1 ambiguities are found.

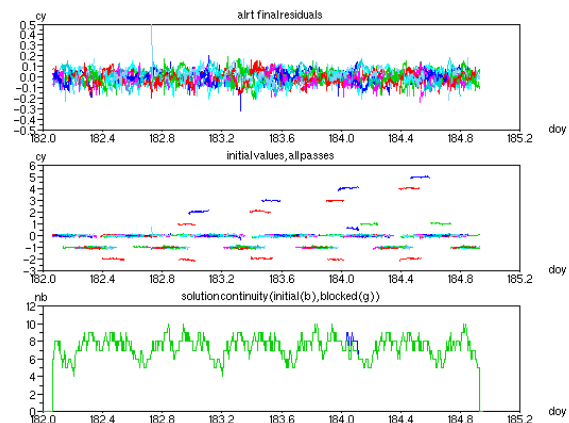


Figure 8: alrt results

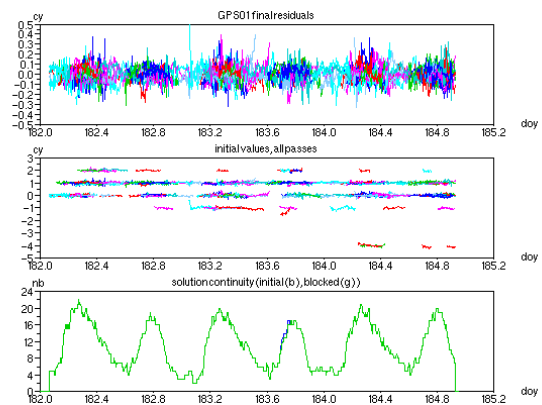


Figure 9: GPS01 results

The comparison of this clock solution with the precise IGS clock solution is performed by aligning the two solutions with a bias for each satellite (due to the unknown remaining integer values in N_w and N_1), and a common offset at each epoch (due to different clock references between the two solutions). The eclipsing satellites and GPS29 were not used in this comparison.

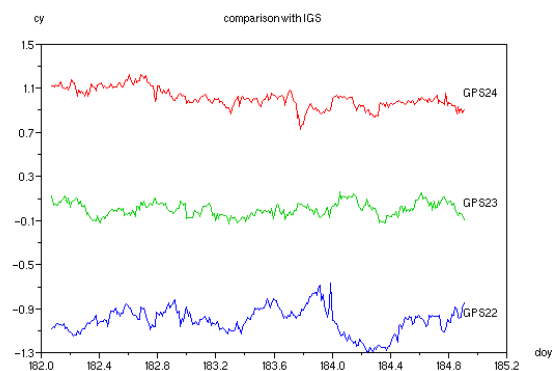


Figure 10 : difference with IGS clock solution

Figure 10 shows the remaining error on a few satellites (a constant offset was added on each curve to clarify the

drawing). Figure 11 shows the histogram of the remaining errors for all processed satellites (no eclipsing satellites). The root mean square of the residuals is 1 cm.

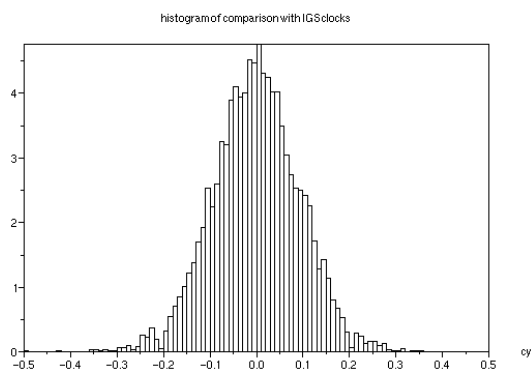


Figure 11 : histogram of differences with IGS clock solution

The performance of this phase solution is very good when compared to the IGS solution.

The integer phase clocks have also the property of fixing zero difference N_1 integer ambiguities on any ground station (using these satellite clocks it is possible to perform integer PPP solutions ref [8]). Figure 12 shows the statistics of the residuals obtained using these integer clocks, applied on $opmt$, which was not in the reference network. These residuals are computed using the floating PPP geometry (for troposphere delay), and before final N_1 fixing.

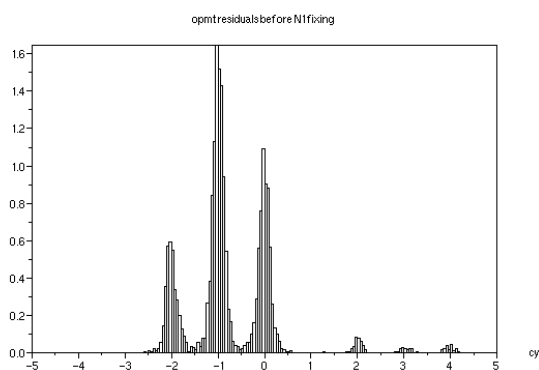


Figure 12 : statistics of zero difference residuals $opmt$, before N_1 fixing

5. CONCLUSION

A complete solution of the zero-difference ambiguity solution for dual frequency systems like GPS has been presented and validated.

Pseudo-range and phase measurements are first used to fix the zero-difference integer widelane ambiguity. This process can be conducted independently at receiver level, because no geometrical model is needed. Only the satellite widelane fractional biases are needed. These

biases have been analysed for year 2007, and are very stable: a daily value is sufficient to achieve an efficient widelane ambiguity blocking.

When these integer widelane values are applied, the global system is equivalent to a single frequency system without ionosphere effects and a wavelength of 10.7 cm.

The remaining zero-difference ambiguity is fixed by solving simultaneously for clocks and ambiguities. The precise IGS ephemerides are used for the models. The complete application on a global network of 54 stations has been presented.

The output of the process is a set of integer phase clocks. The obtained solution is very close to the final IGS clock solution. The precision is sufficient to directly observe the yaw error of eclipsing block IIA satellites in the residuals.

These integer phase clocks have also very interesting properties: they allow absolute integer PPP at receiver level, they are defined modulo 10.7 cm, and have no frequency bias. This is very useful to remove clock discontinuities when connecting overlapping solutions.

6. REFERENCES

1. M. J. Gabor, "GPS Carrier phase Ambiguity, Resolution Using Satellite-Satellite Single Differences", *ION GPS 1999*
2. J. Delporte, F. Mercier, D. Laurichesse, "GPS carrier phase time transfer using single-difference integer ambiguity resolution", *IJNO special issue TimeNav*, Fall 2008
3. J. Delporte, F. Mercier, D. Laurichesse, and O. Galy, "Fixing integer ambiguities for GPS carrier phase time transfer" in *Proceedings of the IEEE International Frequency Control Symposium (IFCS '07)*, pp. 927–932, Geneva, Switzerland, May 2007
4. F. Mercier, D. Laurichesse, "Receiver/Payload hardware biases stability requirements for undifferenced Widelane ambiguity blocking", *Scientifics and fundamental aspects of the Galileo program Colloquium*, Fall 2007, Toulouse, France
5. P. Collins, "Isolating and estimating undifferenced GPS interger ambiguities", *ION NTM 2008*, January 2008, San Diego, Californie.
6. J. Ray and K. Senior, "IGS/BIPM pilot project: GPS carrier phase for time/frequency transfer and timescale formation," *Metrologia*, vol. 40, no. 4, p. 205, 2003.
7. J. Delporte, F. Mercier, D. Laurichesse, "Time Transfer using GPS Carrier Phase with Zero- Difference Integer Ambiguity Blocking", *EFTF-08*, Toulouse, April 2008

8. D. Laurichesse, F. Mercier, "Integer ambiguity resolution on undifferenced GPS phase measurements and its application to PPP", *ION-GNSS 2007*, Fort Worth, Texas

9. D. Laurichesse, F. Mercier, J.P. Berthias, J. Bijac, "Real Time Zero-difference Ambiguities Blocking and Absolute RTK" *ION NTM 2008*, January 2008, San Diego, Californie

10. J.M. Dow, R.E. Neilan, G. Gendt, "The International GPS Service (IGS): Celebrating the 10th Anniversary and Looking to the Next Decade," *Adv. Space Res.* 36 vol. 36, no. 3, pp. 320-326, 2005. doi:10.1016/j.asr.2005.05.125